

## Sensor integration

**UV Light Detection With Side Polished CYTOP Fiber**

Ada Ayechu<sup>1</sup>, Desiree Santano<sup>1</sup> , Juan David López Vargas<sup>2</sup> , Ignacio R. Matias<sup>1,3\*</sup> , and Ignacio del Villar<sup>1,3</sup>

<sup>1</sup>Department of Electrical, Electronic and Communication Engineering, Public University of Navarra, 31009 Pamplona, Spain

<sup>2</sup>Nanotechnology Engineering Program, Federal University of Rio de Janeiro, Rio de Janeiro 21941-901, Brazil

<sup>3</sup>Institute of Smart Cities, Public University of Navarra, 31009 Pamplona, Spain

\*Fellow, IEEE

Manuscript received 17 June 2023; revised 11 July 2023; accepted 20 July 2023. Date of publication 1 August 2023; date of current version 14 August 2023.

**Abstract**—Cyclic transparent optical polymer (CYTOP) fiber, used mainly in strain detection and refractive index characterization of liquids, can be polished for the detection of ultraviolet (UV) light radiation. The study investigates the transmission spectra of CYTOP fiber exposed to different intensities of UV light, demonstrating a linear relationship. A simplified system using a single wavelength, i.e., 395 nm, shows real-time performance of the sensor in a range from 1 to 15 mW. The results reveal the potential of CYTOP fiber as a UV sensor with a sensitivity of 0.65%/mW and a limit of detection of 0.3 mW, offering implications for monitoring UV radiation exposure and related health risks. In addition, the effect of the UV light was also observed at longer wavelengths with a lower intensity variation, which suggests that CYTOP fiber could be used for transmitting the UV radiation detection in telecommunications bands.

**Index Terms**—Sensor integration, Optical sensors, cyclic transparent optical polymer (CYTOP) optical fiber, intensity sensor, side polishing, ultraviolet (UV) light.

**I. INTRODUCTION**

Plastic optical fibers have attracted much interest during the last decades in sensors domain due to their high elastic strain limits, high fracture toughness, high flexibility in bending, high sensitivity to strain, and potential negative thermo-optic coefficients [1]. More specifically, fluorinated polymers have gained prominence due to their remarkable properties, such as high transparency, thermal stability, and infrared transmission [2], [3], [4], [5].

Within fluorinated optical fibers, cyclic transparent optical polymer (CYTOP) fiber has been widely used, mainly for Bragg gratings-based measurements [6], [7]. In addition, CYTOP fiber, thanks to the low refractive index it presents, i.e., 1.34–1.35 [8], very close to water, allows a high evanescent field to be obtained when tapered. Hence, a high sensitivity to the surrounding medium refractive index is obtained [9]. This idea is something common in many optical fiber sensors: When the refractive index of the substrate is very similar to the surrounding medium [10], it increases drastically and this is why CYTOP fiber is very adequate for applications where molecules in liquid must be detected, because liquids typically show a refractive index very similar to water.

Another way to potentiate the sensitivity of CYTOP fiber is by lateral polishing and a further deposition of a gold thin film [11], which permits the achievement of a sensitivity higher than 20 000 nm per refractive index unit in a refractive index close to water.

Here, we aim to explore the effect of ultraviolet (UV) light on the transmission of light through CYTOP fiber. Building upon previous findings that showcased spectral variations in the fiber when exposed to gamma radiation [12], [13], our focus now shifts toward comprehending the effects of UV light. With the utmost significance placed on human wellbeing, the accurate monitoring of UV radiation exposure from both natural sunlight and artificial light sources becomes

imperative. The potential consequences of excessive UV exposure are far reaching, extending beyond mere sunburns to include an increased risk of developing skin cancer [14]. Hence, our exploration of UV light's influence on light transmission through a side polished CYTOP fiber serves to deepen our understanding of the mechanisms behind UV-related health risks. According to a study performed with a PMA2100 radiometer in Coimbatore, India, UVB irradiance was maximum between 12.00 noon–1.00 P.M. (19.50–40.2  $\mu\text{W}/\text{cm}^2$ ) and UVA between 12 noon–1.15 P.M. (4.70–6.59 mW/cm<sup>2</sup>) [15], whereas in [14], a sensor for real-time monitoring of UV in a range from 0.1 to 10 mW was developed. This indicates the range of values necessary to detect.

**II. EXPERIMENTAL SETUP**

For the fabrication of the proposed UV sensor, a CYTOP plastic optical fiber (GigaPOF120SR, Thorlabs) with a 120  $\mu\text{m}$  core and 490  $\mu\text{m}$  cladding was utilized. To expose the evanescent field, it was necessary to perform a side polishing on the CYTOP fiber. To reduce the final roughness of the CYTOP fiber after polishing, side polishing was performed using three different types of sandpaper. Initially, silicon carbide sandpaper with a grit size of 2000 was used, followed by sandpaper with a finer grit size of 5000. Finally, a 3- $\mu\text{m}$  aluminum oxide polish film (Fiber Instrument Sales) was applied. The outcome of this process is a D-shaped side polishing, with the most polished section having a final thickness of 243  $\mu\text{m}$  (initially 490  $\mu\text{m}$ ), as depicted in Fig. 1(a).

After that, the optical fiber was included in the setup depicted in Fig. 1(b), where one end was connected to a broadband source (an ASBN-W—high power series white light source from Spectral Products Inc.) and the other end to an HR4000 spectrometer (OceanOptics Inc., Largo, FL, USA). In addition to this, a fiber-coupled LED light source emitting at 395 nm was oriented to the polished side of the fiber UV light source so that UV light is coupled to the light transmitted and detected by the spectrometer. In addition, in order to calibrate the

Corresponding author: Ignacio del Villar (e-mail: [ignacio.delvillar@unavarra.es](mailto:ignacio.delvillar@unavarra.es)).

Associate Editor: J. Bong (JB) Lee.

Digital Object Identifier 10.1109/LSENS.2023.3300828

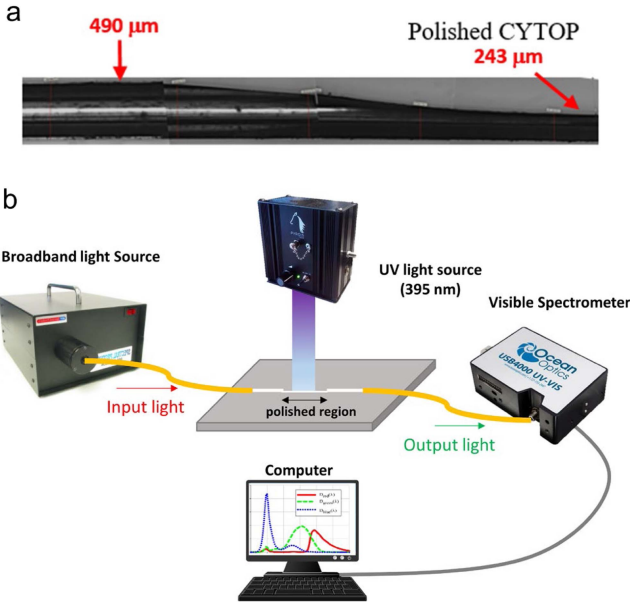


Fig. 1. Photograph of the side polished CYTOP fiber and experimental setup where UV light couples to the light transmitted by a broadband source emitting in the visible range.

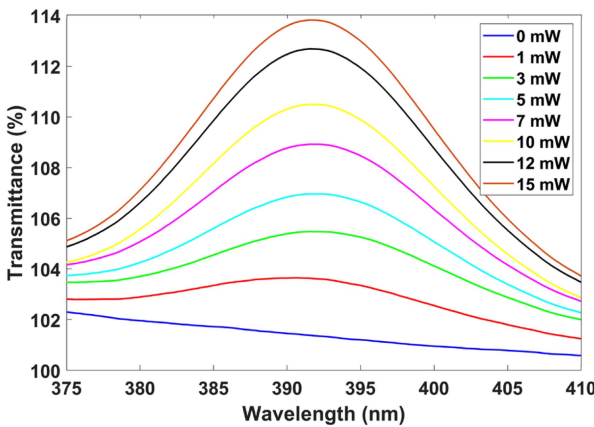


Fig. 2. Variation of the transmittance at 395 nm when UV light from a LED source emitting at 395 nm couples to the light transmitted by a broadband source emitting in the visible and near infrared range.

signal detected by the spectrometer, a laser photodiode with a wide spectral range (200–1100 nm), model PD300-UV P/N7Z02413 from Ophir Photonic, was used. This permitted the monitoring of the optical signal intensity in milliwatts.

### III. RESULTS

Fig. 2 shows the transmission spectra monitored by the spectrometer in the range from 375 to 410 nm for different intensities of the UV LED source ranging from 0 to 15 mW. Light from the UV LED source is coupled to the CYTOP fiber in an apparent linear way. In Fig. 2, the signal is not centered exactly at 395 nm due to the tolerance of the central wavelength of the LED source (LZ1-00UB00), which is 5 nm according to the manufacturer. In addition, there are other factors that can affect, such as temperature.

In order to simplify the system, Fig. 3 shows the variation of the transmittance monitored by the spectrometer at 395 nm. Although

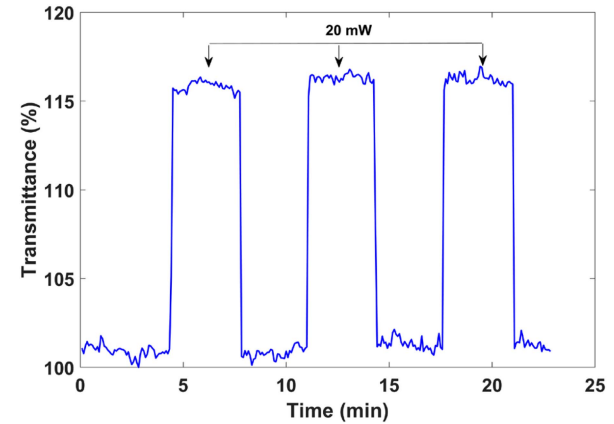


Fig. 3. Transmittance of the polished CYTOP at 395 nm when exposed to UV light with a power of 20 mW.

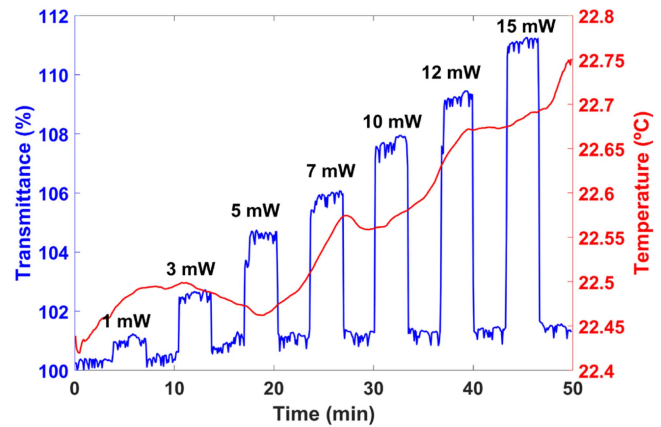


Fig. 4. Transmittance at 395 nm when UV light from an LED source emitting at 395 nm couples to the light transmitted by a broadband source emitting in the visible and near infrared range. The polished CYTOP was exposed to UV light with a power ranging from 1 to 15 mW. The red line shows also the temperature.

the experimental setup in Fig. 1 is based on a broadband source and a spectrometer, analyzing the performance for a single wavelength certified the capability of the system to consist of an LED source and a photodetector at the same time a real-time signal can be shown, not discrete values as in Fig. 2. In Fig. 3, three measurements were conducted with the UV light directed onto the polished side of the fiber at a power level of 20 mW. The measurement was repeated three times in order to demonstrate that the process is quite repeatable. Moreover, the 15% variation in the transmittance agrees well with the linear fit that will be shown in Fig. 6.

Fig. 4 goes one step forward and shows the real-time performance of the sensing system for the same intensity values used for the spectral analysis in Fig. 2. In Fig. 4, it was possible to discriminate the different intensities with a drift that is due to the variation of the temperature during the experiment. CYTOP fiber is sensitive to temperature, as demonstrated in other works [16], [17]. This effect was not observed in Fig. 3 where the temperature was quite stable (the laboratory where the experiments were performed controls temperature with  $\pm 1^\circ\text{C}$  error so there are time slots with more or less variations).

Hence, the ambient temperature was monitored with a negative temperature coefficient (NTC) thermistor during the experiment. This way, the drifts induced by temperature are compensated by a minimum error algorithm. First, as the sampling frequencies of the temperature

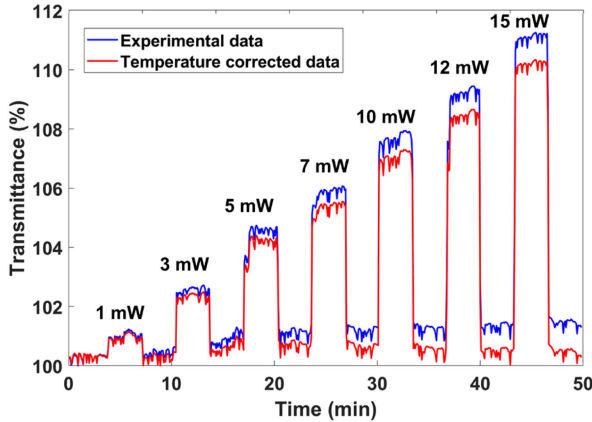


Fig. 5. Transmittance at 395 nm when UV light from an LED source emitting at 395 nm couples to the light transmitted by a broadband source emitting in the visible and near infrared range. The blue line shows the raw data and the red the corrected values after application of a temperature compensation algorithm.

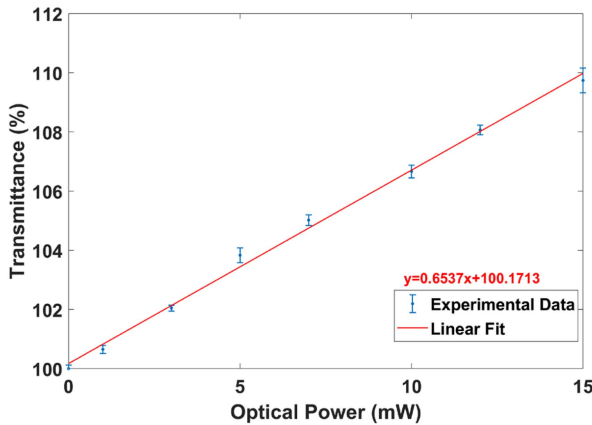


Fig. 6. Calibration displayed together with the linear fit of the experimental points. The proposed UV sensor achieved a sensitivity of 0.65%/mW.

sensor and that of the spectrometer do not match, it is necessary to resample, in this case, the one of higher frequency, so we do not need to interpolate data. Then, a correction factor is calculated, which corresponds to the ratio of the maximum increment of the spectra base line, that is, not considering the detection peaks, by the maximum increment of the temperature. Finally, at each increment, the spectrum data are corrected by extracting from the experimental data the amount corresponding to the difference of the temperature at that increment minus the minimum temperature, and this difference multiplied by the correction factor in order to translate the change in temperature to the change in transmittance of the spectrum. Fig. 5 compares the signal with and without temperature correction.

In addition, in Fig. 6, it is possible to contrast the variation of the transmittance in Fig. 5, observed for the seven different UV intensities, with a linear fit-based calibration curve (the correlation coefficient  $R^2$  was 0.9959). The limit of detection was estimated following the method explained in [18], where the limit of detection was calculated as the blank mean value plus three times the standard deviation of the blank. With this method, a limit of detection of 0.3 mW was obtained, which indicates that intensities lower than 1 mW can be detected, with a sensitivity of 0.65%/mW. Furthermore, no filtering process of

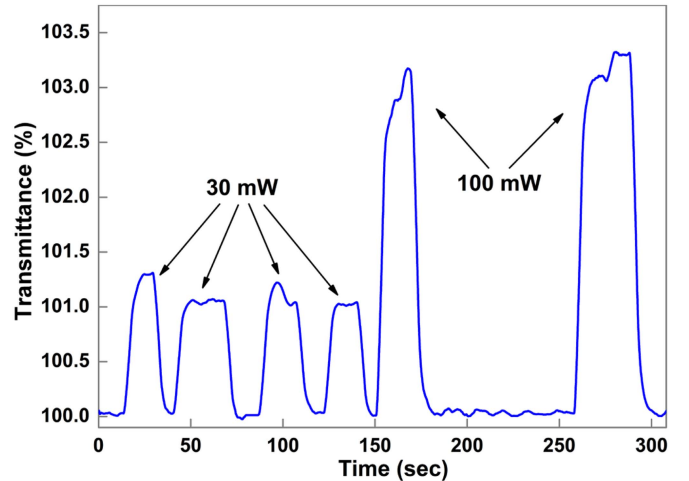


Fig. 7. Transmittance at 700 nm when UV light from an LED source emitting at 395 nm couples to the light transmitted by a broadband source emitting in the visible and near infrared range.

the signal was performed, which suggests that a much lower limit of detection can be achieved.

Finally, Fig. 7 shows the signal obtained when monitoring the variation of the transmittance under the same setup where a broadband source is emitting light and an LED source emitting at 395 nm is placed in front of the polished side of the optical fiber. The particularity here is that the transmittance is monitored at 700 nm, which demonstrates the capability of the system to monitor the UV light radiation at wavelengths different from the UV radiation.

In Fig. 7, the two values that were monitored are 30 and 100 mW, and it is evident that the variation of the signal is lower than at 395 nm, at the same time it was necessary to apply an algorithm to reduce the noise. This lower signal response confirms the idea that in terms of selectivity it is better to monitor the UV wavelengths, where more signal variation is attained. On the other hand, the detection at longer wavelengths opens the path to distributed sensing in a similar way to fiber Bragg gratings (FBGs) when applied at different points of a fiber in structural health monitoring, for instance. Polishing the fiber at different points of a fiber would permit to monitor de UV radiation in an extended area. Obviously, the challenge is to multiplex the signal, because the setup presented here is an intensity based and not a wavelength resonance-based one. However, this could be solved by using FBGs in CYTOP fiber, since each FBG would lead to a resonance band centered at a specific wavelength, avoiding an overlap of the signals corresponding to each side polished region of the fiber.

#### IV. CONCLUSION

This study investigated the influence of UV light on light transmission through CYTOP fiber, revealing its potential as a UV sensor for monitoring UV radiation exposure and understanding related health risks. The experimental setup involved side polishing of the CYTOP fiber and coupling UV light using a fiber-coupled LED source. Spectrometer analysis showed a linear relationship between UV light intensity and transmittance, with slight temperature-related drifts compensated using an algorithm. The UV sensor was calibrated, exhibiting high sensitivity (0.65%/mW) and a detection limit of 0.3 mW. These findings highlight CYTOP fiber as a reliable and sensitive UV sensor.

The implications of this research are significant for human well-being, as accurate and real-time monitoring of UV radiation is crucial for mitigating health risks, including skin cancer. CYTOP fiber presents a promising solution in this regard. Furthermore, the study revealed the detection of variations at 700 nm wavelength. The variations of the signal are reduced at this wavelength (only 30 and 100 mW radiation could be discriminated), but this opens the path for detecting UV light and coupling this signal to the signal transmitted in telecommunications network.

Overall, this study deepens our understanding of UV light's effects on CYTOP fiber's light transmission and provides a viable approach for developing high-sensitivity UV sensors. Further research can focus on refining the sensor design, the stability of the sensitivity after exposure to UV power or the reproducibility of the experiments (the polishing degree is critical in terms of acceptance of coupling UV light, and it must be controlled very precisely) optimizing the signal processing techniques, and exploring potential applications in areas such as environmental monitoring, industrial safety, and personal UV exposure tracking. By harnessing the capabilities of CYTOP fiber, we can better protect individuals from the harmful effects of UV radiation and promote healthier living environments.

## ACKNOWLEDGMENT

This work was supported by the Spanish Agencia Estatal de Investigación (AEI) through Project PID2019-106231RB-I00. The work of Desirée Santano was supported by the Public University of Navarre through a predoctoral research grant. The work of Juan David López-Vargas was supported by the Coordenação de Aperfeiçoamento de Pessoal de Nível Superior - Brasil (CAPES) - Finance Code 001 ("doutorado sanduiche").

## REFERENCES

- [1] K. Peters, "Polymer optical fiber sensors-a review," *Smart Mater. Struct.*, vol. 20, no. 1, 2011, Art. no. 013002, doi: [10.1088/0964-1726/20/1/013002](https://doi.org/10.1088/0964-1726/20/1/013002).
- [2] V. F. Cardoso, D. M. Correia, C. Ribeiro, M. M. Fernandes, and S. Lanceros-Méndez, "Fluorinated polymers as smart materials for advanced biomedical applications," *Polymers*, vol. 10, no. 2, pp. 1–26, 2018, doi: [10.3390/polym10020161](https://doi.org/10.3390/polym10020161).
- [3] S. Wang, T. Liu, X. Wang, Y. Liao, J. Wang, and J. Wen, "Hybrid structure Mach-Zehnder interferometer based on silica and fluorinated polyimide microfibers for temperature or salinity sensing in seawater," *Meas. J. Int. Meas. Confederation*, vol. 135, pp. 527–536, 2019, doi: [10.1016/j.measurement.2018.11.036](https://doi.org/10.1016/j.measurement.2018.11.036).
- [4] Y. Mao et al., "Optical oxygen sensors based on microfibers formed from fluorinated copolymers," *Sensors Actuators, B Chem.*, vol. 282, pp. 885–895, 2019, doi: [10.1016/j.snb.2018.11.143](https://doi.org/10.1016/j.snb.2018.11.143).
- [5] X. Xu, M. Luo, J. Liu, and N. Luan, "Fluorinated polyimide-film based temperature and humidity sensor utilizing fiber Bragg grating," *Sensors*, vol. 20, no. 19, 2020, Art. no. 5469, doi: [10.3390/s20195469](https://doi.org/10.3390/s20195469).
- [6] A. G. Leal-Junior et al., "Simultaneous measurement of axial strain, bending and torsion with a single fiber Bragg grating in CYTOP fiber," *J. Lightw. Technol.*, vol. 37, no. 3, pp. 971–980, 2019, doi: [10.1109/JLT.2018.2884538](https://doi.org/10.1109/JLT.2018.2884538).
- [7] A. Theodosiou and K. Kalli, "Recent trends and advances of fibre Bragg grating sensors in CYTOP polymer optical fibres," *Opt. Fiber Technol.*, vol. 54, 2020, Art. no. 102079, doi: [10.1016/j.yofte.2019.102079](https://doi.org/10.1016/j.yofte.2019.102079).
- [8] K. Takeya, Y. Ikegami, K. Matsumura, K. Kawase, and H. Uchida, "Optical evaluation of CYTOP, an amorphous fluoropolymer, in the terahertz frequency across a wide temperature range," *Appl. Phys. Exp.*, vol. 12, no. 4, 2019, Art. no. 042004, doi: [10.7567/1882-0786/ab0716](https://doi.org/10.7567/1882-0786/ab0716).
- [9] R. Gravina, G. Testa, and R. Bernini, "Perfluorinated plastic optical fiber tapers for evanescent wave sensing," *Sensors*, vol. 9, no. 12, pp. 10423–10433, 2009, doi: [10.3390/s91210423](https://doi.org/10.3390/s91210423).
- [10] A. Urrutia, I. Del Villar, P. Zubiate, and C. R. Zamarreño, "A comprehensive review of optical fiber refractometers: Toward a standard comparative criterion," *Laser Photon. Rev.*, vol. 13, no. 11, 2019, Art. no. 1900094, doi: [10.1002/lpor.201900094](https://doi.org/10.1002/lpor.201900094).
- [11] S. Cao et al., "Highly sensitive surface plasmon resonance biosensor based on a low-index polymer optical fiber," *Opt. Exp.*, vol. 26, no. 4, 2018, Art. no. 3988, doi: [10.1364/oe.26.003988](https://doi.org/10.1364/oe.26.003988).
- [12] A. Leal-Junior et al., "Influence of gamma and electron radiation on perfluorinated optical fiber material composition," *Mater. Lett.*, vol. 340, 2023, Art. no. 134205, doi: [10.1016/j.matlet.2023.134205](https://doi.org/10.1016/j.matlet.2023.134205).
- [13] I. Chapalo, A. Gusarov, D. Kinet, K. Chah, Y.-G. Nan, and P. Megret, "Postirradiation transmission characteristics of CYTOP fiber exposed by gamma radiation," *IEEE Trans. Nucl. Sci.*, vol. 69, no. 4, pp. 656–662, Apr. 2022, doi: [10.1109/TNS.2022.3148986](https://doi.org/10.1109/TNS.2022.3148986).
- [14] J. Tian, Y. He, J. Li, J. Wei, G. Li, and J. Guo, "Fast, real-time, in situ monitoring of solar ultraviolet radiation using sunlight-driven photoresponsive liquid crystals," *Adv. Opt. Mater.*, vol. 6, no. 6, 2018, Art. no. 1701337, doi: [10.1002/adom.201701337](https://doi.org/10.1002/adom.201701337).
- [15] S. Balasaraswathy, P. Kumar, U. Srinivas, and C. R. Nair, "UVA and UVB in sunlight, optimal utilization of UV rays in sunlight for phototherapy," *Indian J. Dermatol. Venereology Leprology*, vol. 68, no. 4, pp. 198–201, 2002.
- [16] Y. Zheng, K. Bremer, and B. Roth, "Investigating the strain, temperature and humidity sensitivity of a multimode graded-index perfluorinated polymer optical fiber with Bragg grating," *Sensors*, vol. 18, no. 5, 2018, Art. no. 1436, doi: [10.3390/s18051436](https://doi.org/10.3390/s18051436).
- [17] Y.-G. Nan, D. Kinet, K. Chah, I. Chapalo, C. Caucheteur, and P. Mégrét, "Ultra-fast fiber Bragg grating inscription in CYTOP polymer optical fibers using phase mask and 400 nm femtosecond laser," *Opt. Exp.*, vol. 29, no. 16, 2021, Art. no. 25824, doi: [10.1364/oe.428592](https://doi.org/10.1364/oe.428592).
- [18] F. Chiavaioli, C. A. Gouveia, P. A. Jorge, and F. Baldini, "Towards a uniform metrological assessment of grating-based optical fiber sensors: From refractometers to biosensors," *Biosensors*, vol. 7, no. 2, 2017, Art. no. 23, doi: [10.3390/bios7020023](https://doi.org/10.3390/bios7020023).